Biochemical Pharmacology 82 (2011) 1843–1852

Contents lists available at SciVerse ScienceDirect

Biochemical Pharmacology

journal homepage: www.elsevier.com/locate/biochempharm

# Cytotoxicity and cell death mechanisms induced by the polyamine-vectorized anti-cancer drug F14512 targeting topoisomerase II

Viviane Brel *, Jean-Philippe Annereau, Stéphane Vispé, Anna Kruczynski, Christian Bailly, Nicolas Guilbaud

*Centre de Recherche en Oncologie Expérimentale, Institut de Recherche Pierre Fabre, Centre de Recherche et Développement, 3 Avenue Hubert Curien, BP 13562, 31035 Toulouse cedex 1, France*

ARTICLE INFO

*Article history:*
Received 30 June 2011
Accepted 31 August 2011
Available online 8 September 2011

*Keywords:*
F14512
Etoposide
Polyamines
Topoisomerase II
Apoptosis
Senescence

ABSTRACT

The polyamines transport system (PTS) is usually enhanced in cancer cells and can be exploited to deliver anticancer drugs. The spermine-conjugated epipodophyllotoxin derivative F14512 is a topoisomerase II poison that exploits the PTS to target preferentially tumor cells. F14512 has been characterized as a potent anticancer drug candidate and is currently in phase 1 clinical trials. Here we have analyzed the mechanisms of cell death induced by F14512, compared to the parent drug etoposide lacking the polyamine tail. F14512 proved to be >30-fold more cytotoxic than etoposide against A549 non-small cell lung cancer cells and triggers less but unrecoverable DNA damages. The cytotoxic action of F14512 is extremely rapid (within 3 h) and does not lead to a marked accumulation in the S-phase of the cell cycle, unlike etoposide. Interestingly, A549 cells treated with F14512 were less prone to undergo apoptosis (neither caspases-dependent nor caspases-independent pathways) or autophagy but preferentially entered into senescence. Drug-induced senescence was characterized qualitatively and quantitatively by an increased β-galactosidase activity, both by cytochemical staining and by flow cytometry. A morphological analysis by electron microscopy revealed the presence of numerous multi-lamellar and vesicular bodies and large electron-lucent (methuosis-like) vacuoles in F14512-treated cell samples. The mechanism of drug-induced cell death is thus distinct for F14512 compared to etoposide, and this difference may account for their distinct pharmacological profiles and the markedly superior activity of F14512 in vivo. This study suggests that senescence markers should be considered as potential pharmacodynamic biomarkers of F14512 antitumor activity.



## 1. Introduction

Despite the approval over the past ten years of several targeted therapeutic drugs – mainly kinase inhibitors and monoclonal antibodies – cytotoxic agents continue to play a major role in cancer chemotherapy. Novel cytotoxic drugs have been approved recently (e.g. ixabepilone, vinflunine, trabectedin, eribulin) and newer drug candidates active against resistant cancers are regularly proposed and tested in the clinic. Drugs specifically vectorized to cancer cells should offer a reinforced activity, to tackle tumor cells while preserving normal cells, resulting in an improved therapeutic index and/or reducing unwanted toxicities. In this context, attempts have been made to target drugs to cancer cells based on the elevated and specific need of polyamines for cancer cells proliferation [1–3]. The selective targeting of tumor cells with polyamine-containing drugs has been considered [4–7] and the most promising compound in this category is arguably the spermine–podophyllotoxin conjugate F14512.

F14512 is a polyamine-targeted cytotoxic drug that contains a spermine chain in place of the C4 glycosidic moiety of etoposide (Fig. 1). This polyamine conjugate displays an enhanced anti-proliferative activity on a large panel of tumor cell lines as compared to etoposide and exploits the polyamines transport system (PTS) to accumulate into cells [8]. For example, PTS-deficient cells are significantly less sensitive to F14512 than PTS-positive cells [8]. The potent antitumor activity of F14512 against a panel of 18 tumor xenografts has been robustly demonstrated,

*Abbreviations:* AML, acute myeloid leukemia; ATP, adenosine tri-phosphate; BSA, bovine serum albumin; DMSO, dimethyl sulfoxide; DNA, deoxyribonucleic acid; DSB, double-strand breaks; $EC_{50}$, half maximal effective concentration; FBS, fetal bovine serum; MAP-LC3, microtubule-associated protein-light chain 3; MEM, minimum essential medium; PBS, phosphate buffer saline; PS, phosphatidyl serine; PTS, polyamine transport system; SA-β-GAL, senescence associated β galactosidase.

* Corresponding author. Tel.: +33 5 34 50 60 79; fax: +33 5 34 50 30 54.
*E-mail addresses:* viviane.brel@pierre-fabre.com, vsbrel@hotmail.com (V. Brel), jean.philippe.annereau@pierre-fabre.com (J.-P. Annereau), stephane.vispe@pierre-fabre.com (S. Vispé), anna.kruczynski@pierre-fabre.com (A. Kruczynski), christian.bailly@pierre-fabre.com (C. Bailly), nicolas.guilbaud@pierre-fabre.com (N. Guilbaud).

0006-2952/$ – see front matter © 2011 Elsevier Inc. All rights reserved.
doi:10.1016/j.bcp.2011.08.028

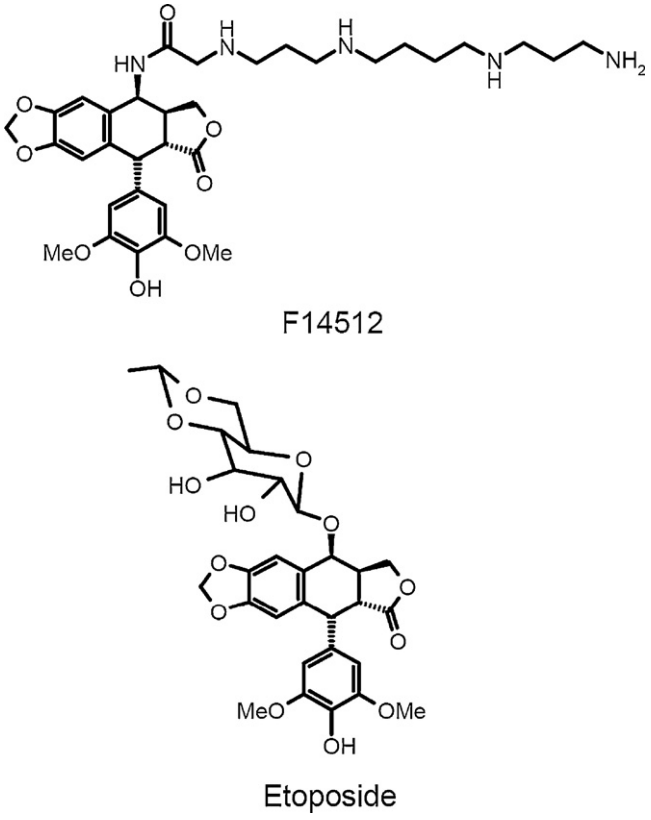


**Fig. 1.** Structures of F14512 and etoposide.

with significant responses in 67% of the tumor models evaluated [9]. In another study, we established a clear correlation between the expression of the PTS system in 13 leukemia cell lines and their sensitivity to the cytotoxic action of F14512 [10]. This observation has encouraged the set up of a phase 1 clinical study with F14512 in patients with acute myeloid leukemia (AML). Moreover, a spermine-based fluorescent probe [11] has been designed and tested to identify PTS-positive tumor patients [10]. The phase 1 trial of F14512 in AML is on-going.

At the molecular level, the spermine tail of F14512 contributes to (i) enhance the water solubility of the drug, (ii) target the PTS in cancer cells and (iii) reinforce the activity of the drug toward its primary molecular target, topoisomerase II. Indeed, a recent study demonstrated that F14512 functions as a powerful topoisomerase II poison capable of stabilizing topoisomerase II–DNA covalent complexes much more efficiently than etoposide [12]. A preferential inhibitory activity toward the α isoform of the enzyme has been observed although the drug stimulates DNA cleavage mediated by both human topoisomerase IIα or topoisomerase IIβ. The enhanced activity of F14512 correlates with a tighter binding and an increased stability of the ternary topoisomerase II–drug–DNA complex [12].

In order to determine how these molecular properties translate at the cellular level, we have compared the action of F14512 vs etoposide in terms of cytotoxicity, kinetic of inhibition of cell proliferation, cell cycle modulation and cell death pathways, using the A549 non-small cell lung cancer cell line as a representative PTS-positive cell model particularly sensitive to F14512 [8]. A particular attention was paid to elucidating the cell death pathway exploited by F14512 as it may represent a key aspect of the pharmacological profile of this drug candidate. Recent reports suggested that DNA-damaging agents or topoisomerase II inhibitors (including etoposide) can induce alternative cell death such as cellular senescence [13] or the formation of vesicules of autophagy [14]. Moreover, spermine can induce autophagy alone [15] or when coupled with a DNA-damaging agent such as the naphtilimide–polyamine conjugate NPC-16 [7]. This aspect is of main interest for F14512 as the compound displays an original kinetic response in vivo, as compared with etoposide. The maximal antitumor effect of F14512 demonstrated in the xenograft MX-1 breast cancer model appears after the end of the treatment period, suggesting that F14152 induced strong and irreversible impact on cellular proliferation associated with a delayed cell death [9]. These considerations prompted us to examine the mechanism of cell death – apoptosis, autophagy and senescence – triggered by F14512 in A549 cells. As recommended in the guidelines for cell death studies [16–18], we performed at least two complementary technical approaches to evaluate the extent of drug-induced apoptosis, senescence or autophagy in order to decipher the cell death pathway induced by F14512 at different time-points.

## 2. Materials and methods

### 2.1. Chemicals and drugs

F14512 was provided by Pierre Fabre Medicament (Castres, France) and etoposide was purchased from SICOR (Cortegaça, Portugal). The design and synthesis of F14512 have been patented (WO 2005/100363). F14512 and etoposide were first dissolved in DMSO and used in cellular assays at a maximal final DMSO concentration of 0.1%.

### 2.2. Cell culture

A549 (lung carcinoma) cells were cultivated in MEM supplemented with 5% FBS, 2 mM L-glutamine, 100 μg/mL penicillin-streptomycin and 1.25 μg/mL fungizone (amphotericine B). Cells were incubated at 37 °C in a humidified atmosphere with 5% $CO_2$ and maintained using standard cell culture techniques.

### 2.3. Antiproliferative activity

The antiproliferative activity of test compounds was measured using the ATPlite assay (Perkin Elmer) on A549 cells. Cells were seeded in 96 well plates ($10^3$ cells/well), incubated for 24 h to obtain a subconfluent monolayer and then treated with increasing concentrations of test compounds. Cell viability was evaluated by dosing the ATP released by viable cells after 3, 6, 24, 48 and 72 h incubation period. For a second experiment, cells were seeded and treated as described above. After each incubation period, cells were washed with PBS and incubated with culture medium for a total time period of 72 h. The antiproliferative activity was then analyzed as described above.

### 2.4. Cell cycle analysis

A549 cells were seeded in T75-flasks ($10^6$ cells for 24 h and 48 h treatment, $0.7 \times 10^6$ for 72 h treatment) and incubated with 6 different concentrations ranging from 0.125 to 4 fold the $IC_{50}$ value (determined in the ATPlite assay) for 24, 48 and 72 h at 37 °C in a 5% $CO_2$ controlled atmosphere. Cells were then rinsed twice with PBS, collected with a solution of trypsin-like enzyme and resuspended in PBS. Cells were fixed and stained using the Kit Coulter DNA-Prep Reagents (Beckman Couter, Miami, FL), following the manufacturer's protocol. The fluorescence intensity emitted from propidium iodide–DNA complexes was finally acquired by a FACS XL-4 Beckman analyzer. Percentages of cells in each cell-cycle phase were calculated using M Cycle software.

### 2.5. DNA double-strand breaks detection

A549 cells were seeded in 12-wells plates ($3 \times 10^5$ cells/well) and cultured for 24 h. Cells were then exposed to increasing concentrations of F14512 and etoposide for 4 h. For the detection of DNA double-strand breaks (DSBs), cells were fixed and permeabilized with DNA-Prep LPr Reagent (Beckman Coulter), blocked with Bovine Serum Albumin 1% in PBS, stained with an Alexa Fluor 647 anti-H2AX-phosphorylated (ser139) antibody (Biolegend) for 45 min and washed with PBS containing 1% BSA. For the DNA content analysis, cells were stained 1 h with DNA-Prep STAIN Reagent. Phospho-H2AX positive cells were analyzed on a FACS Aria cytometer (BD Biosciences).

### 2.6. Annexin V-PE/Nexin-7AAD staining experiments

A549 cells were seeded in 12-well plates ($7 \times 10^4$ cells/well) and treated with increasing concentrations of tested compounds for 16 h. Cells were then trypsinized and stained with the Guava PCA-96 Nexin kit (Guava Technologies, Hayward, CA) according to the manufacturer's protocol. This kit contains Annexin V coupled with phycoerythrin and 7-amino actinomycin D (7-AAD) that binds to intracellular nucleic acid when the membrane integrity is impaired. Thereafter, samples were analyzed with a Guava PCA-96 flow cytometer.

### 2.7. Caspases 3/7 activation measurements

A549 cells were seeded on a 96-well plate ($6 \times 10^3$ cells/well). After 24-h incubation, cells were treated with different concentrations of F14512 and etoposide and incubated at 37 °C in a 5% $CO_2$ controlled atmosphere for 16 h. Caspases 3/7 enzyme activities were measured using the Caspase-Glo 3/7 assay (Promega Corp., Madison, WI), following the manufacturer's instructions.

### 2.8. Measurements of mitochondrial transmembrane potential ($\Delta\Psi m$)

The fluorescent cation dye JC-1 was used for $\Delta\Psi$m determination. Briefly, cells were treated with DMSO, F14512 or etoposide ($10^{-5}$, $10^{-6}$ and $10^{-7}$ M) overnight. Control and treated cells were harvested, incubated with 1 μg/mL JC-1 at 37 °C for 30 min, washed and resuspended in PBS containing SYTOX Red Dead cell stain (5 ng/mL). Samples were analyzed by flow cytometry (FACS Aria, BD Biosciences).

### 2.9. MAP-LC3 B immunofluorescence

Cells were treated 24–72 h, harvested, fixed in 4% paraformaldehyde, permeabilized in ice-cold methanol (90%), saturated in PBS 0.5% BSA and stained with anti-LC3B monoclonal antibody (CellSignaling Ref 3868S), followed by a Alexa Fluor 488-conjugated secondary antibody. Cells were either observed by fluorescence microscopy (Axioskop Zeiss) or analyzed by flow cytometry (FACS Aria, BD Biosciences).

### 2.10. Transmission electron microscopy

A549 cells were fixed with 2% glutaraldehyde in 0.1 mol/L Sorensen phosphate buffer (pH 7.4) for 4 h at 4 °C and washed with Sorensen phosphate buffer (0.2 M) for 12 h at 4 °C. Cells were then post-fixed with 1% $OsO_4$, 0.25 mol/L saccharose, 0.05 mol/L Sorensen phosphate buffer. Cells were washed twice with distilled water and pre-stained with a 2% uranyl acetate solution for 12 h. After dehydratation, ultrathin sections were mounted on 150 mesh collodion-coated copper grids and post-stained with 3% uranyl acetate in 50% ethanol and with 8.5% lead citrate for observation under an H300 (HU12A) Hitachi electron microscope (25–125 kV).

### 2.11. Cytochemical assay of SA-β-Gal activity

A549 cells were seeded in 24-well plates ($7.5 \times 10^3$ cells/well). After a 72 h exposure with F14512 or etoposide, cells were washed, fixed and stained with the Senescence cells histochemical staining kit (Sigma) following the manufacturer's protocol. Cells were observed with a Axioskop Zeiss microscope.

### 2.12. C12–FDG assay of SA-β-Gal activity

A549 cells were seeded in 24-well plates ($1.5 \times 10^4$ cells/well). After a 72 h exposure with F14512 or etoposide, cells were washed twice with PBS, incubated 80 min with 25 μM C12-FDG, washed with PBS, harvested and analyzed by flow cytometry (Guava PCA-96 flow cytometer).

### 2.13. Statistical analysis

All experiments were performed at least three times. $EC_{50}$ values were determined with curve fitting analysis (non linear regression model with a sigmoidal dose response, variable hill slope coefficient), performed with the algorithm provided by the GraphPad Software (GraphPad Software Inc., CA, USA). Comparisons between F14512 and etoposide treated samples were made using a paired two-tailed *t*-test. $p < 0.05$ was considered statistically significant.

## 3. Results

### 3.1. Antiproliferative activity

We have previously demonstrated that F14512 was 35-fold more cytotoxic than etoposide in A549 cells [8]. To extend this observation, we compared the kinetic of activity of both compounds using the same cell line. As shown in Fig. 2A, both F14512 and etoposide induced a time- and dose-dependent cytotoxicity, with a noticeable growth inhibitory effect observed after 48 h treatment. After 6 or 24 h treatment, the two drugs behave more or less similarly but after 48 or 72 h, major differences can be observed; F14512 being considerably more potent than etoposide. $EC_{50}$ values were calculated: $9.1 \times 10^{-8}$ M and $1.3 \times 10^{-8}$ M (with 95% confidence intervals [$3.5 \times 10^{-8}$ to $2.4 \times 10^{-7}$ M] and [$8.2 \times 10^{-9}$ to $2.1 \times 10^{-8}$ M]) for F14512 and $1.2 \times 10^{-6}$ M and $4.1 \times 10^{-7}$ M (with 95% confidence intervals [$3 \times 10^{-7}$ to $4.8 \times 10^{-6}$ M] and [$2.4 \times 10^{-7}$ to $7 \times 10^{-7}$ M]) for etoposide after a 48 and 72 h treatment, respectively. As the ATPlite assay is based on the cellular metabolic activity which can be decreased not only by cell death but also by quiescence and senescence, we have confirmed these results by cell counting (data not shown). $EC_{50}$ values were $4.6 \times 10^{-8}$ M and $1.2 \times 10^{-6}$ M after 48 h and $2.6 \times 10^{-8}$ M and $4.1 \times 10^{-7}$ M after 72 h for F14512 and etoposide respectively. In these experiments, the vectorized drug F14512 exhibits a very significant advantage in term of anti-proliferative potency ($p = 0.004$ and 0.001 after 48 h and 72 h respectively).

To assess whether the cytotoxic effect was transient or irreversible, another kinetic experiment was performed. After drug exposure (for 3, 6, 24, 48 or 72 h), F14512 and etoposide were replaced by drug-free media and cells were incubated for a total time period of 72 h. For each time point, the percentage of proliferation inhibition was calculated at the dose corresponding to the $EC_{50}$ of the drug after a 72 h treatment (Fig. 2B). A 3 h exposure to F14512 was sufficient to induce a significant irreversible impact on cell proliferation (29% vs 7% for etoposide). Etoposide required a longer

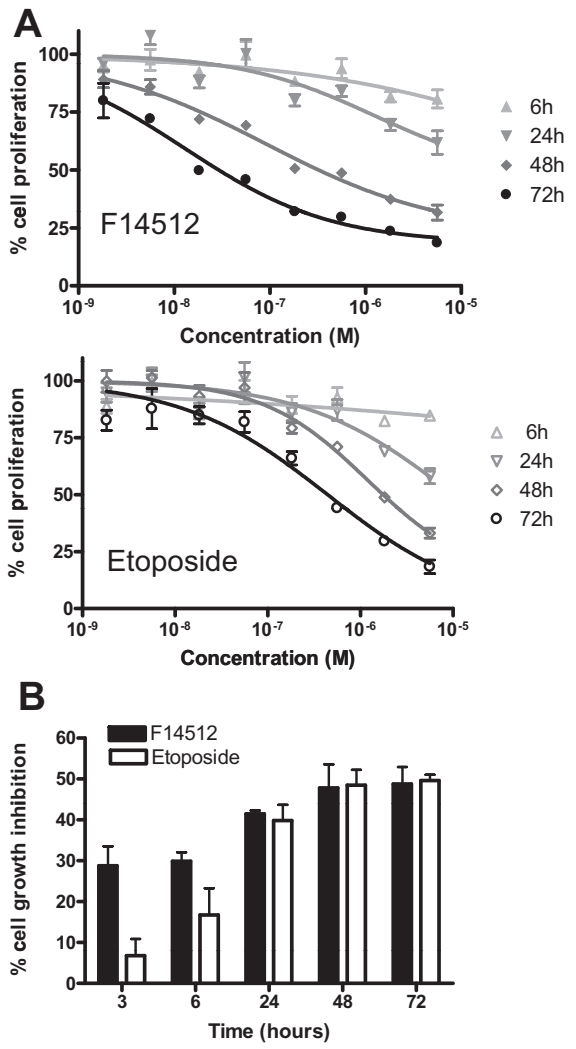


**Fig. 2.** Anti-proliferative effect of F14512 and etoposide on A549 cells. A. Measurements after an incubation period of 6, 24, 48 and 72 h. B. A549 cells were treated for 6, 24, 48 and 72 h with the test drug (at a concentration corresponding to 1 $EC_{50}$ value), then washed with PBS and incubated with culture medium until a total incubation period of 72 h. In both cases, cell proliferation was analyzed using an ATPlite assay ($n = 3$).

treatment period to reach the same effect than F14512, the two compounds being comparable after 24 h drug exposure. The vectorized-drug seems to enter cells faster than etoposide but F14512 treated cells undergo a longer cell death pathway. It is clear at this stage that the two molecules behave differently.

### 3.2. Cell cycle analysis

We compared the effects of the drug at equicytotoxic concentrations (0.125, 0.25, 0.5, 1, 2 and 4 $IC_{50}$). The FACS analysis (Fig. 3) showed that A549 cells treated with etoposide accumulated massively in S-phase 24 h after treatment (80% at 4 $IC_{50}$), then were blocked in the G2/M phase in a dose-dependent manner (75% at 2 $IC_{50}$) at 48 h treatment. In contrast, the impact of F14512 on the cycle of A549 cells was relatively modest. No S-phase arrest was observed and only 45% G2/M-arrested cells were obtained at 2 $IC_{50}$ after 48 h treatment with F14512.

### 3.3. Drug-induced DNA damages

A key step of the mechanism of action of both F14512 and etoposide is the topoisomerase II-dependent induction of DNA damages, essentially DNA double-strand breaks (DSBs) induced by the enzyme trapped in a covalent complex. DSBs manifest by phosphorylation of histone H2AX on Ser-139 which is mediated by protein kinases of the phosphoinositide-3 kinase family (ATM, ATR, and/or DNA-PK). The presence of Ser-139 phosphorylated H2AX (γH2AX) is thus a reporter of DNA damage [19]. We analyzed the induction of DSBs by flow cytometry, calculating the percentage of phospho-H2AX positive A549 cells. At equicytotoxic doses, both compounds induced DNA-damage in a dose-dependent manner (Fig. 4). After a 4 h incubation period, the percentages of stained cells are significantly lower under treatment with F14512 compared to etoposide treated cells. For example, at a dose of etoposide corresponding to 5 $IC_{50}$ (5 μM) the % of H2AX-positive cells is considerably higher than the % observed upon treatment with a dose of 1 μM F14512 which corresponds to 75 $IC_{50}$ (Fig. 4). It is clear that F14512 induces much less DNA damage than etoposide, despite its higher cytotoxicity [8] and superior capacity to interfere with topoisomerase II in vitro [12].

### 3.4. Drug-induced apoptosis

Induction of apoptosis was first evaluated via the conventional annexin V-PE/7-AAD staining procedure. Exposure of phosphatidyl serine residues (PS) on the external surface of the cell membrane usually occurs at early stages of apoptotic cell death and can be readily measured by flow cytometry. With A549 cells, F14512 showed a minimal effect, with an $EC_{50}$ of 3.7 μM. As shown in Fig. 5A, only a small proportion of Annexin V positive and 7-AAD negative cells (18%) was detected after 16 h exposure to F14512 for concentrations up to $10^{-5}$ M. On the opposite, etoposide induced a dose-dependent increase in early apoptotic cells with an $EC_{50}$ ($9.4 \times 10^{-7}$ M) close to its antiproliferative $EC_{50}$ value and significantly different ($p = 0.014$) from the $EC_{50}$ of F14512.

We further investigated the apoptotic pathways measuring the two effector caspases 3 and 7 activities after 16 h drug exposure (Fig. 5B). F14512 induced a dose-dependent increase of caspases-3/7 activity only at high doses (above 3 μM), when etoposide exhibited a dose response correlated with its cytotoxicity ($EC_{50}$: 5.1 μM). In other words, the extent of apoptosis induced by etoposide is consistent with its level of cytotoxicity but this is not the case with F14512. In this assay, the two compounds are significantly different in term of potency ($p = 0.01$). To extend these observations, we next assessed whether and to what extent the two drugs might have an effect on the mitochondrial membrane potential ($\Delta\Psi m$) by using the mitochondrion specific dye JC-1. The flow cytometric analysis showed (Fig. 5C) that F14512 did not induce any mitochondrial membrane depolarization when tested at doses up to 10 μM while etoposide exhibited a modest but noticeable dose-dependent depolarization (21.5% cells with a depolarized mitochondrial membrane under 10 μM etoposide vs 6.8% with 10 μM F14512 with A549 cells). Altogether, these data indicate that F14512 does not behave as a pro-apoptotic agent, in contrast to etoposide, at least in this cell context.

### 3.5. Drug-induced autophagy

Autophagy is an alternative cell death mechanism often reported for cytotoxic drugs. To examine this alternative non-apoptotic pathway, we first observed F14512- and etoposide-treated A549 cells by electron microscopy, to search for the potential formation of characteristic autophagic vacuoles bounded by a double membrane. Typical images are presented in Fig. 6A. No typical double membrane structures were observed with cells treated with any of the two drugs. Fig. 6A shows cells treated for 48 h with 10 μM etoposide or F14512 but we also tested a range of drug concentrations and different time of exposure to the

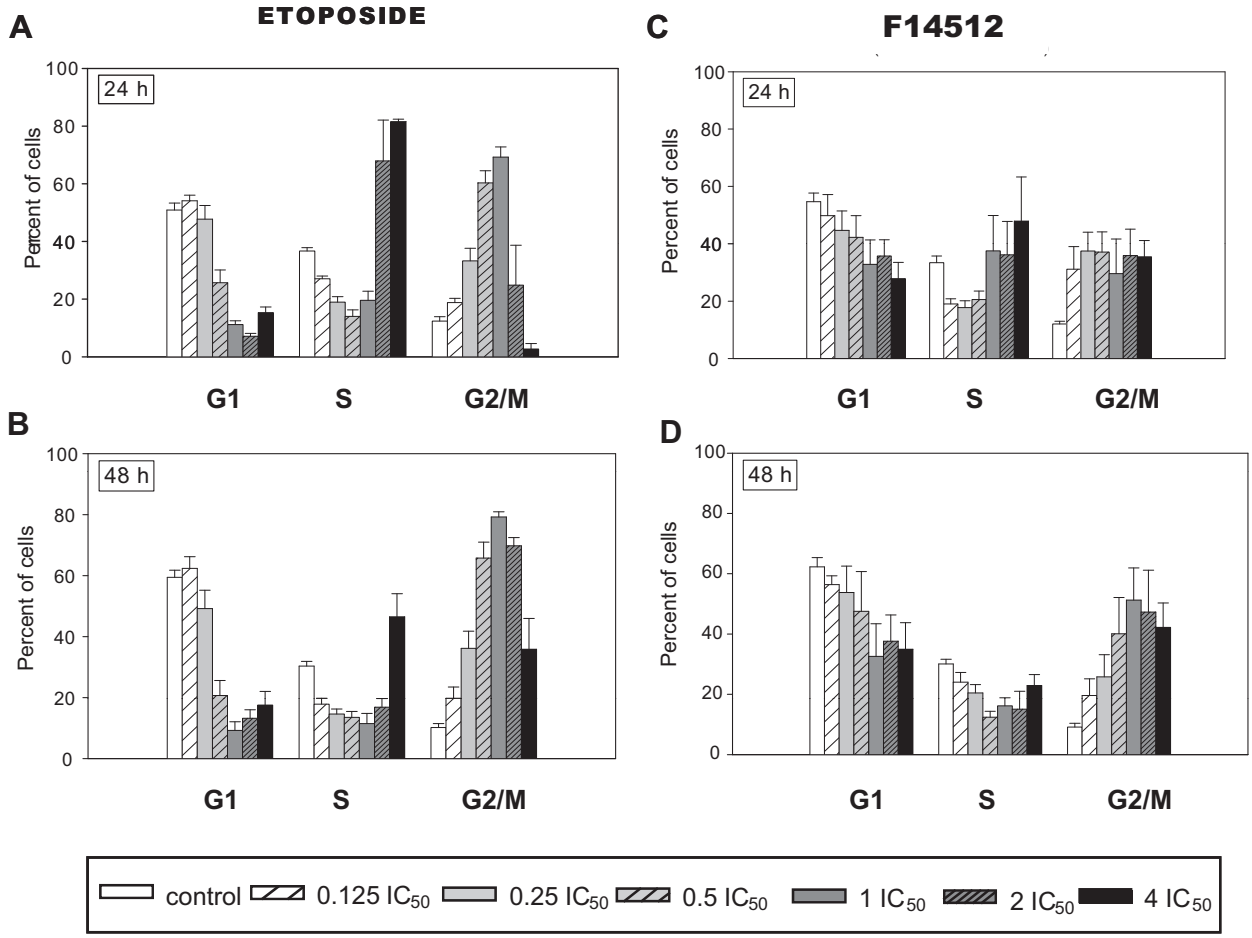


**Fig. 3.** Cell cycle analysis of A549 cells treated with F14512 or etoposide. A549 cells were exposed to equi-cytotoxic doses of F14512 or etoposide for 24 and 48 h. Cells were harvested and labelled with the Kit Coulter DNA-Prep reagents. After a 1 h incubation, cells were analyzed by flow cytometry ($n = 3$).

compounds (24, 48 and 72 h). However, interestingly a difference was noticed between the two drugs. We observed the presence of numerous multilamellar bodies in the drug-treated cell samples compared to the controls. The extent of cytoplasmic vacuolization was significantly more important with F14512 compared to etoposide. But these vacuoles are not derived from autolysosomes. Indeed, to assess whether these intracytoplasmic structures signed an autophagic degradation of organelles, we performed an immunofluorescence assay using the lipid-conjugated form of MAP-LC3 (LC3-II) that localizes on the membrane of autophagosomes. The microtubule associated protein light-chain 3 (LC3) is a well established autophagosome marker which exists in a cytosolic form (LC3-I) and a form that is conjugated to phosphatidylethanolamine on autophagosome membranes (LC3-II) [20]. As shown in Fig. 5B, no LC3-II labelling was observed in etoposide or F14512 treated cells, even at high doses (up to 30 μM) for incubation periods ranging from 24 to 72 h. Yet, reference compounds (positive controls) such as tamoxifen or rapamycin induced a clear punctuated LC3-II labelling of autophagic vacuoles. We thus conclude that the two drugs do not induce autophagic cell death. The cytoplasmic vacuolization phenomenon, prominent with F14512, may sign another cell death mechanism.

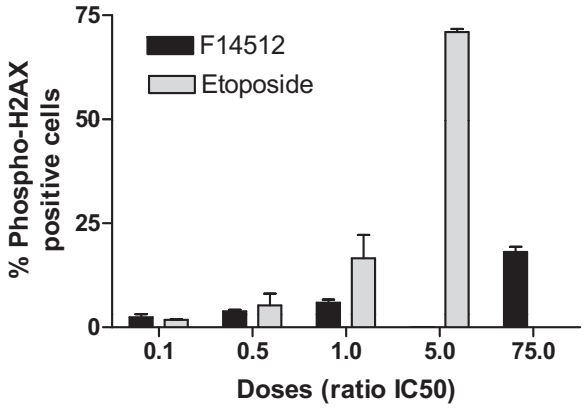


**Fig. 4.** DNA damage induced by equi-cytotoxic doses of F14512 and etoposide. A549 cells were incubated for 4 h with increasing doses of F14512 or etoposide. Cells were then fixed, permeabilized and stained with an anti-phospho-H2AX antibody. Phospho-H2AX positive cells were quantified by flow cytometry ($n = 3$).

### 3.6. Drug-induced senescence

As a third potential mechanism of drug-induced cell death, we examined cellular and biochemical markers of senescence. To test this hypothesis, we first performed a senescence-associated-β-galactosidase (SA-β-Gal) cytochemical staining of F14512- and etoposide-treated A549 cells (Fig. 7A). After 48 h drug exposure, cells exhibited an enlarged and flattened morphology with a typical blue coloration, at doses above $10^{-7}$ M and $10^{-6}$ M for F14512 and etoposide, respectively. The blue color formation of substrate X-Gal (5-bromo-4-chloro-3-indolyl-β-D-galactopyranoside) inside cells determines the presence of SA-β-galactosidase positive cells. This qualitative assay attests unambiguously of the induction of senescence by F14512. Next, to quantify the difference between these two drugs, we used the fluorescent probe C12-FDG

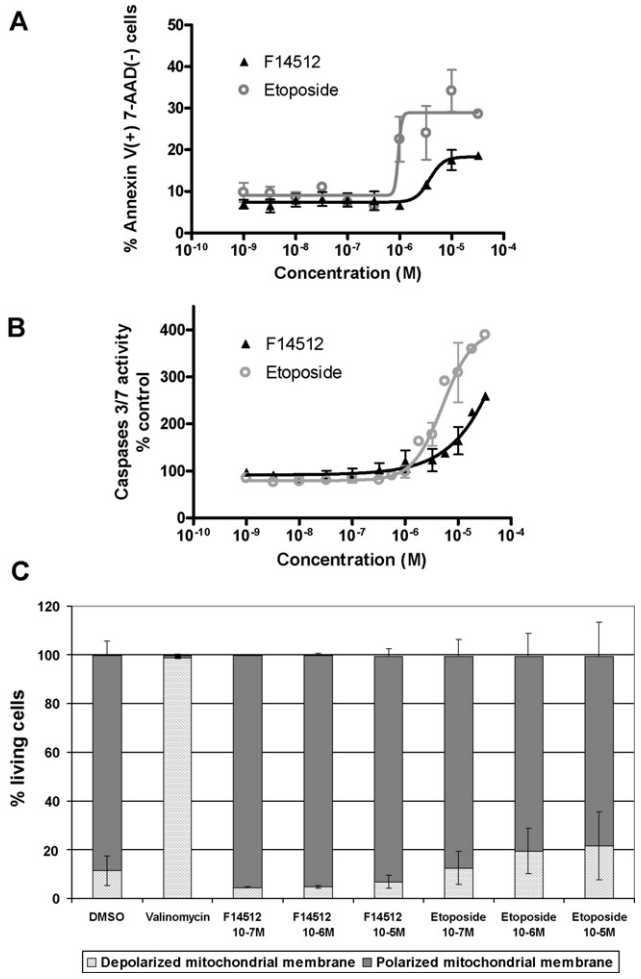


**Fig. 5.** Apoptosis induced by F14512 and etoposide. (A) Early apoptosis was assessed by Annexin V and PI staining experiment on A549 cells. Cells were treated for 16 h, trypsinized, stained with the kit Guava PCA-96 Nexin and analyzed by flow cytometry ($n = 3$). (B) Activation of caspases-3/7 in A549 cells. Cells were treated with increasing concentrations of F14512 and etoposide for 16 h. Caspases-3/7 activity was measured using Caspase Glo kit (luminescence) ($n = 4$) (C) Depolarization of mitochondrial membrane in A549 cells. Cells were treated with F14512 or etoposide overnight, and then harvested and stained with the JC-1 dye. Fluorescence was measured by FACS ($n = 3$).

which releases fluorescein when hydrolysed by SA-β-Gal [21,22]. C12-FDG is a more sensitive lipophilic version of fluorescein-di-β-D-galactopyranoside (FDG) which is a useful substrate for β-galactosidase, capable of entering into viable cells and giving a fluorescence emission proportional to the enzymatic activity. We analyzed the dose effects after 72 h treatment by flow cytometry (Fig. 7B). Both compounds exhibited a dose response with F14512 being considerably (14-fold) more potent than etoposide ($EC_{50} = 1.85 \times 10^{-8}$ M and $2.6 \times 10^{-7}$ M, respectively) (Fig. 7B). The $p$ value ($p = 0.0002$) attests that the difference between the two drugs is extremely significant. The $EC_{50}$ measured in this senescence-based assay with F14512 is comparable to the $EC_{50}$ determined in the cytotoxicity assay. These later experiments characterize F14512 as a potent senescence inducer.

## 4. Discussion

This study provides several novel information important to better understand the mechanism of action of the drug candidate F14512 at the cellular level. First, the higher cytotoxic potency of F14512 compared to etoposide is clearly illustrated here using the A549 non-small cell lung cancer cell line. Not only F14512 is >30-fold more cytotoxic than etoposide but also the anti-proliferative activity occurs more rapidly. F14512 caused an irreversible anti-proliferative impact after short exposure times and with a delayed cell death response (Fig. 2). It takes longer with etoposide to exert its anti-proliferative potential. This is certainly the reflect of the PTS exploited by F14512, but not by etoposide, for accumulating into A549 cells. We have shown previously that the PTS is highly expressed in A549 cells [8]. Logically, a more rapid accumulation of F14512 into A549 cells would be responsible for a quicker anti-proliferative effect. However, the delayed response is noticeable with F14512 and could be in contradiction with the vectorization principle. In fact, the polycationic spermine moiety provides the compound with a good affinity for polyanionic structures either in the cytoplasm or in the nucleus (such as its target DNA). Thus, it may modify the intracellular distribution of F14512. Another explanation of the delayed response observed in our anti-proliferative assays could be the sequestration of the polyamine-conjugated drug in cytoplasmic vesicles. Indeed, it has been reported that a polyamine tethered to the fluorophore bodipy accumulates in acidic vesicles into the cytoplasm and is then released in the cytosol [23]. This latter step is relatively slow. Both the kinetics and the targets of the drug could then be modified by the vectorization. However, the intrinsic molecular mechanism can also be invoked to some extent. It is noticeable that F14512 is more active against topoisomerase IIα than topoisomerase IIβ [12] and topoisomerase IIα is known to trigger the cytotoxic response of various compounds including etoposide [24,25]. Moreover, the A549 cellular model preferentially expresses the α isoform than the β isoform topoisomerase II gene [26]. Topoisomerase IIα is essential for cell proliferation and is highly expressed in vigorously growing cells, whereas topoisomerase IIβ is non-essential for growth [27,28]. Therefore, it is conceivable that both the PTS and the topoisomerase IIα inhibitory activity of F14512 contribute to the more rapid cytotoxic action compared to etoposide. Interestingly, a similar rapid kinetic of cytotoxic response has been described with the synthetic benzophenanthridine alkaloid NK314, which is a specific topoisomerase IIα inhibitor [24,29].

F14512 is an extremely potent targeted cytotoxic agent, active against a large panel of cancer cell lines [8,10] and tumor xenografts [9]. But surprisingly, despite a prominent inhibition of topoisomerase II [12], F14512 induced much less DNA damage than etoposide, as demonstrated here in the cellular phospho-H2AX assay (Fig. 3) and previously using a Comet assay [8]. Here again, to explain this particularity we may invoke the relative selectivity of F14512 for the α isoform rather than β isoform of topoisomerase II, the latter being involved in etoposide-induced DSBs and DNA rearrangements [23]. But there are certainly other explanations, as yet not entirely elucidated. However, at this stage we can mention a very recent work performed with a Drosophila model showing that, in addition to its topoisomerase II inhibitory properties, F14512 has the unique ability, over other topoisomerase II poisons tested (including etoposide), to interact with specific DNA targets, modulating the expression of a discrete group of genes [30]. We have now accumulated several lines of evidences clearly showing that F14512 behaves distinctly from etoposide and, to some extent, the cell cycle data also corroborate this conclusion. Etoposide induces cell cycle delay, principally in the S and G2/M-phases, the major cell cycle phases of DNA damage and repair. At this point, our results with etoposide on A549 cells recapitulated the data from the literature [31–33]. F14512 exerts a much less pronounced effect at the cell cycle level, consistent with the induction of less (but certainly more lethal) DNA damage. Indirectly, this suggests that the contribution of the polyamine tail of the conjugate could play multiple roles in terms of cell transport, target inhibition and cancer cell death.

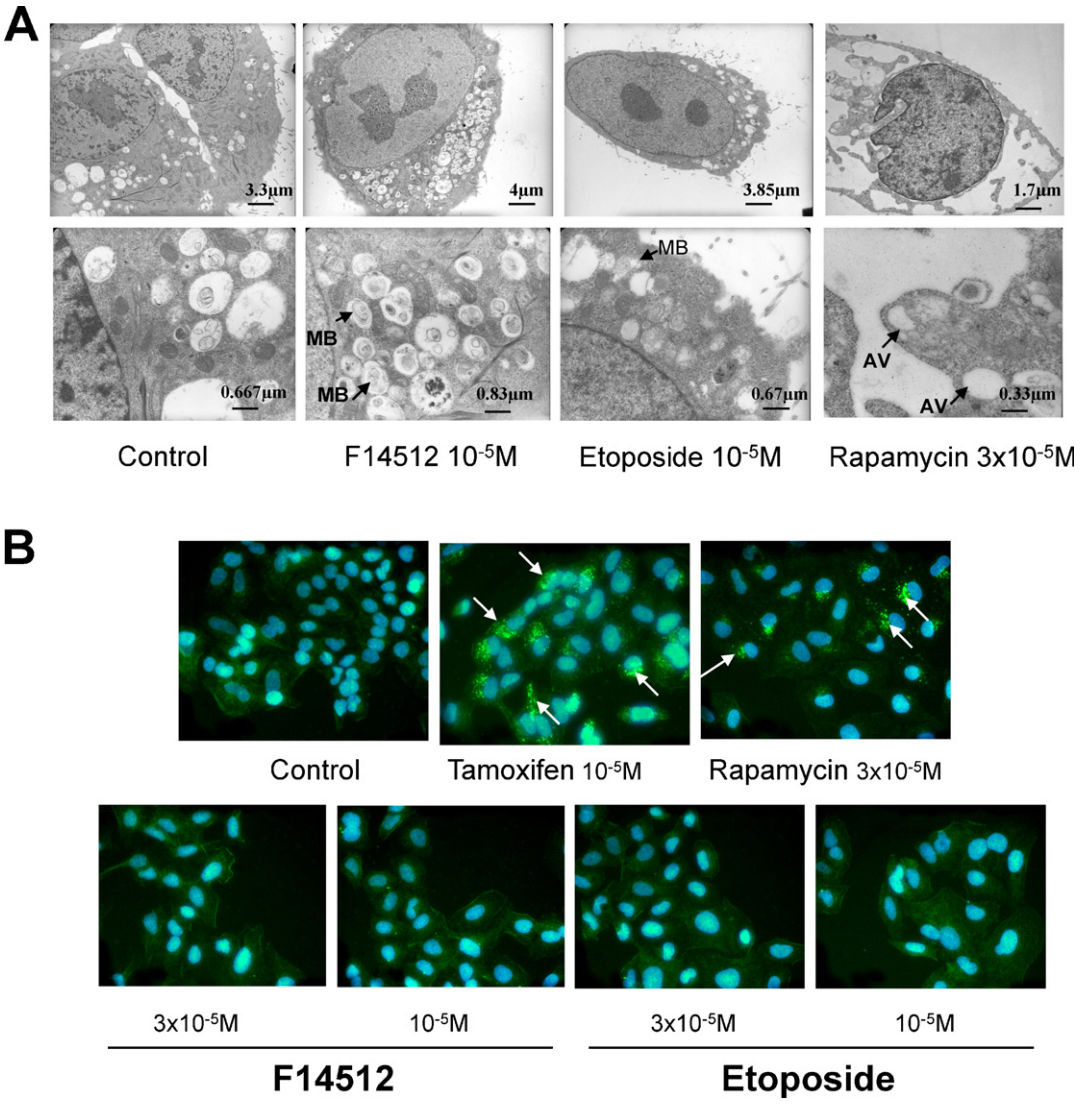


**Fig. 6.** Autophagy induced by F14512 and etoposide. Electron microscopy of A549 cells treated with F14512 or etoposide for 48 h (MB: multilamellar bodies; AV: autophagic vacuoles) ($n = 2$) (A). A549 cells were treated with increasing concentrations (3 nM to 30 μM) of F14512 or etoposide for 24 h, fixed, permeabilized and stained with anti MAP-LC3B antibody. Autophagic vacuoles (white arrows) were analyzed by fluorescence microscopy ($n = 3$) (B).

The cell death mechanism induced in F14512-treated cancer cells was investigated here for the first time. Cell death triggered by topoisomerase poisons has been described for several years [34,35] and the crucial role of apoptosis in etoposide-induced cytototoxicity is well-documented [36–38]. If etoposide is usually categorized as a major pro-apoptotic anti-cancer drug, clearly this is not the case for F14512. In a previous in vivo study, we noticed that F14512 activated caspase-3 expression in a MX-1 xenograft of breast cancer [9] but in vitro the drug always give little sign of apoptosis. Our experiments performed for up to 48 h with three complementary assays showed only at high concentrations of F14512 a moderate caspase-dependent apoptosis signal. Consistently under the same experimental conditions, no effect on the mitochondrial apoptotic pathway was noticed. In contrast, etoposide induced apoptosis at doses corresponding to the anti-proliferative effective doses. This is not surprising in fact, as the relationship between etoposide-induced cell cycle changes and variations of the mitochondrial membrane potential or apoptosis is well known. The arrest in the G2/M phase of the cells treated with low concentrations of etoposide is associated with an increase in the potential of mitochondrial membranes whereas treatment with higher drug concentration trigger massive apoptosis and a collapse of $\Delta\Psi m$ [39]. In contrast, F14512 induces little cell cycle changes, minor DNA damage in cells (quantitatively), and then does not behave as a pro-apoptotic effector.

Recently, many papers described alternative cell death pathways induced by etoposide such as autophagy [14,40]. Moreover, spermidine is also able to induce autophagy [41,42]. However, our results showed that neither etoposide-, nor F14512-treated A549 cells underwent autophagic cell death, as measured by MAP-LC3B labelling for time points up to 72 h (Fig. 6 and data not shown). The analysis by electronic microscopy supported this conclusion, as we did not observe the formation of typical autophagic vesicles with double membranes. As recently published, autophagy could be involved in resistance to etoposide treatment rather than in cytotoxic response [7,43]. Therefore, the absence of biochemical markers of autophagy in A549 could indicate a better cytotoxic response to the F14512 or etoposide treatment.

From the MAP-LC3B labelling data and electron microscopy (EM) observations, the hypothesis that F14512 could induce autophagy was discarded. Nevertheless, the EM is informative and may suggest an alternative form of nonapoptotic cell death. As described for Fig. 6A, treatment of A549 cells with F14512, and to a lower extent with etoposide, leads to an extreme vacuolization and

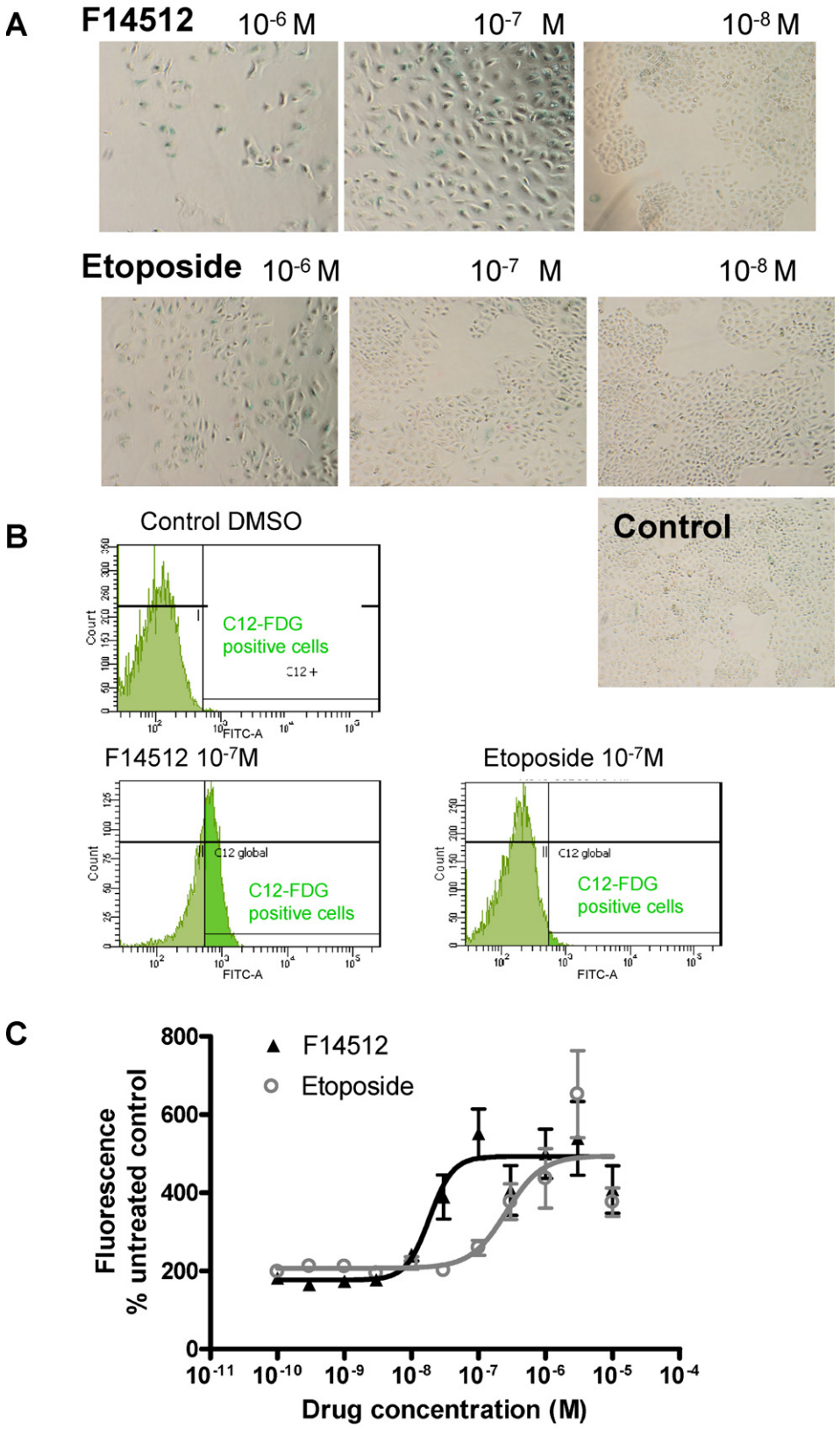


**Fig. 7.** Senescence induced by F14512 and etoposide. Senescence-associated β-galactosidase activity was measured by cytochemical staining (X-gal) in A549 cells treated with F14512 or etoposide for 48 h. Morphological changes and a blue coloration were observed in senescent cells ($n = 3$) (A). FACS analysis of A549 cells treated with F14512 or etoposide (72 h) and incubated with 25 μM C12-FDG. β-Galactosidase hydrolysis of C12-FDG releases fluorescein ($n = 7$) (B and C).

rupture of the cell in some cases. These large vacuoles, generally electron-lucent and devoid of cytoplasmic components, accumulate in the cytoplasm. When observed at a higher magnification (Fig. 6A), these vacuoles seem clearly to have a single membrane and look different from classical autophagosomes [44]. In fact these vacuoles look like those described by Maltese and co-workers for a novel form of cell death designated methuosis (from the Greek methuo, to drink to intoxication) corresponding to an hyperstimulation of vesicular fluid uptake and accumulation of macropinosomes [45,46]. The expansion of macropinocytic vacuoles leads to cell ruptures. By EM, the authors observed numerous lamellipodia closing around regions of extracellular fluid to form nascent macropinosomes in glioblastoma cells [45]. Our images of F14512-treated A549 cells are strangely reminiscent to those morphological descriptions but it is too early to conclude that F14512 can also induce methuosis or another form of nonapoptotic cell death, such as oncosis [47] or paraptosis [48] which also lead to the formation of vacuoles (derived from distended endoplasmic reticulum and/or mitochondria, rather than macropinosomes). It will be useful in the future to dissect further the cell death machinery activated by F14512, knowing however that this is certainly a cell type-dependent and highly adaptable mechanism.

Finally, and this is a salient feature of the work, we demonstrated that F14512 induces senescence at pharmacological doses corresponding to $IC_{50}$ value for anti-proliferative activity while etoposide only triggers this pathway at higher doses. This cell death mechanism is consistent with the observation of a delayed but marked response to F14512 in vivo. Senescence can be viewed as a typical response to DNA damaging agents [49–53]. It has been shown that moderate doses of doxorubicin (another topoisomerase II poison) induced a senescent phenotype in 11/14 cell lines derived from different types of solid tumors [54]. This cell death mechanism was recently proposed as a possible outcome in cancer therapy particularly in apoptosis-refractory tumors [55]. If this proved to be the case for F14512, it could represent a significant advantage for this drug in the clinic. Our present findings also imply that classical apoptosis markers might not be appropriate in following the response to F14512 treatment in tumor patients. Pharmacodynamic markers specific for senescence should be defined and tested. It could be valuable to select potential responders to this anticancer therapy in future clinical trials. For instance, patients exhibiting PTEN negative tumors, which are more sensitive to senescence induction, could take benefit from F14512 treatment [56]. Another option would be to combine F14512 with apoptosis inducing cytotoxic agents that exhibit a different mechanism of action (e.g. with cytarabine in AML) in future clinical protocols in order to target the entire cancer cell population in tumors, sensitive and resistant to apoptosis. Collectively, the present data position F14512 as a spermine-vectorized potent cytotoxic agent capable of inducing cell death by non-apoptotic and senescence-type pathways distinct from those triggered by the parent drug etoposide.

## Acknowledgements

The authors gratefully acknowledge K. André, M.L. Brossard, N. Chansard, L. Lacastaigneratte, N. Novosad and A. Stennevin (CROE-IRPF) for their expert technical assistance. The contributions of the other IRPF members to the synthesis and research on F14512 also are acknowledged.

## References

[1] Scalabrino G, Ferioli ME. Polyamines in mammalian tumors. Part I. Adv Cancer Res 1981;35:151–268.
[2] Scalabrino G, Ferioli ME. Polyamines in mammalian tumors. Part II. Adv Cancer Res 1982;36:1–102.
[3] Palmer AJ, Wallace HM. The polyamine transport system as a target for anticancer drug development. Amino Acids 2010;38:415–22.
[4] Casero Jr RA, Marton LJ. Targeting polyamine metabolism and function in cancer and other hyperproliferative diseases. Nat Rev Drug Discov 2007;6:373–90.
[5] Phanstiel 4th O, Kaur N, Delcros JG. Structure–activity investigations of polyamine–anthracene conjugates and their uptake via the polyamine transporter. Amino Acids 2007;33:305–13.
[6] Tian ZY, Xie SQ, Du YW, Ma YF, Zhao J, Gao WY, et al. Synthesis, cytotoxicity and apoptosis of naphthalimide polyamine conjugates as antitumor agents. Eur J Med Chem 2009;44:393–9.
[7] Xie SQ, Li Q, Zhang YH, Wang JH, Mei ZH, Zhao J, et al. NPC-16, a novel naphthalimide–polyamine conjugate, induced apoptosis and autophagy in human hepatoma HepG2 cells and Bel-7402 cells. Apoptosis 2011;16:27–34.
[8] Barret JM, Kruczynski A, Vispé S, Annereau JP, Brel V, Guminski Y, et al. F14512, a potent antitumor agent targeting topoisomerase II vectored into cancer cells via the polyamine transport system. Cancer Res 2008;68:9845–53.
[9] Kruczynski A, Vandenberghe I, Pillon A, Pesnel S, Goetsch L, Barret JM, et al. Preclinical activity of F14512, designed to target tumors expressing an active polyamine transport system. Invest New Drugs 2011;29:9–21.
[10] Annereau JP, Brel V, Dumontet C, Guminski Y, Imbert T, Broussas M, et al. A fluorescent biomarker of the polyamine transport system to select patients with AML for F14512 treatment. Leuk Res 2010;34:1383–9.
[11] Guminski Y, Grousseaud M, Cugnasse S, Brel V, Annereau JP, Vispé S, et al. Synthesis of conjugated spermine derivatives with 7-nitrobenzoxadiazole (NBD), rhodamine and bodipy as new fluorescent probes for the polyamine transport system. Bioorg Med Chem Lett 2009;19:2474–7.
[12] Gentry AC, Pitts SL, Jablonsky MJ, Bailly C, Graves DE, Osheroff N. Interactions between the etoposide derivative F14512 and human type II topoisomerases: implications for the C4 spermine moiety in promoting enzyme-mediated DNA cleavage. Biochemistry 2011;50:3240–9.
[13] te Poele RH, Okorokov AL, Jardine L, Cummings J, Joel SP. DNA damage is able to induce senescence in tumor cells in vitro and in vivo. Cancer Res 2002;62:1876–83.
[14] Nishida Y, Arakawa S, Fujitani K, Yamaguchi H, Mizuta T, Kanaseki T, et al. Discovery of Atg5/Atg7-independent alternative macroautophagy. Nature 2009;461:654–8.
[15] Madeo F, Eisenberg T, Büttner S, Ruckenstuhl C, Kroemer G. Spermidine: a novel autophagy inducer and longevity elixir. Autophagy 2010;6:160–2.
[16] Klionsky DJ, Abeliovich H, Agostinis P, Agrawal DK, Aliev G, Askew DS, et al. Guidelines for the use and interpretation of assays for monitoring autophagy in higher eukaryotes. Autophagy 2008;4:151–75.
[17] Galluzzi L, Aaronson SA, Abrams J, Alnemri ES, Andrews DW, Baehrecke EH, et al. Guidelines for the use and interpretation of assays for monitoring cell death in higher eukaryotes. Cell Death Differ 2009;16:1093–107.
[18] Kepp O, Galluzzi L, Lipinski M, Yuan J, Kroemer G. Cell death assays for drug discovery. Nat Rev Drug Discov 2011;10:221–37.
[19] Darzynkiewicz Z, Halicka DH, Tanaka T. Cytometric assessment of DNA damage induced by DNA topoisomerase inhibitors. Methods Mol Biol 2009;582:145–53.
[20] Kabeya Y, Mizushima N, Ueno T, Yamamoto A, Kirisako T, Noda T, et al. LC3, a mammalian homologue of yeast Apg8p, is localized in autophagosome membranes after processing. EMBO J 2000;19:5720–8.
[21] Plovins A, Alvarez AM, Ibañez M, Molina M, Nombela C. Use of fluorescein-di-beta-D galactopyranoside (FDG) and C12-FDG as substrates for beta-galactosidase detection by flow cytometry in animal, bacterial, and yeast cells. Appl Environ Microbiol 1994;60:4638–41.
[22] Yang NC, Hu ML. A fluorimetric method using fluorescein di-beta-D-galactopyranoside for quantifying the senescence-associated beta-galactosidase activity in human foreskin fibroblast Hs68 cells. Anal Biochem 2004;325:337–43.
[23] Soulet D, Gagnon B, Rivest S, Audette M, Poulin R. A fluorescent probe of polyamine transport accumulates into intracellular acidic vesicles via a two-step mechanism. J Biol Chem 2004;279(47):49355–66.
[24] Azarova AM, Lyu YL, Lin CP, Tsai YC, Lau JY, Wang JC, et al. Roles of DNA topoisomerase II isozymes in chemotherapy and secondary malignancies. Proc Natl Acad Sci USA 2007;104:11014–9.
[25] Toyoda E, Kagaya S, Cowell IG, Kurosawa A, Kamoshita K, Nishikawa K, et al. NK314, a topoisomerase II inhibitor that specifically targets the alpha isoform. J Biol Chem 2008;283:23711–20.
[26] Gene Expression Omnibus NCBI database (website) http://www.ncbi.nlm.nih.gov/geoprofiles.
[27] Nitiss JL. Targeting DNA topoisomerase II in cancer chemotherapy. Nat Rev Cancer 2009;9:338–50.
[28] Nitiss JL. DNA topoisomerase II and its growing repertoire of biological functions. Nat Rev Cancer 2009;9:327–37.
[29] Onda T, Toyoda E, Miyazaki O, Seno C, Kagaya S, Okamoto K, et al. NK314, a novel topoisomerase II inhibitor, induces rapid DNA double-strand breaks and exhibits superior antitumor effects against tumors resistant to other topoisomerase II inhibitors. Cancer Lett 2008;259:99–110.
[30] Chelouah S, Monod-Wissler C, Bailly C, Barret JM, Guilbaud N, Vispé S, Käs E. An integrated Drosophila model system reveals unique properties for F14512, a. novel polyamine-containing anticancer drug that targets topoisomerase II. PLoS One 2011;6:e23597.

[31] Smith PJ, Souès S, Gottlieb T, Falk SJ, Watson JV, Osborne RJ, et al. Etoposide-induced cell cycle delay and arrest-dependent modulation of DNA topoisomerase II in small-cell lung cancer cells. Br J Cancer 1994;70:914–21.
[32] Potter AJ, Rabinovitch PS. The cell cycle phases of DNA damage and repair initiated by topoisomerase II-targeting chemotherapeutic drugs. Mutat Res 2005;572:27–44.
[33] Knudsen KE, Booth D, Naderi S, Sever-Chroneos Z, Fribourg AF, Hunton IC, et al. RB-dependent S-phase response to DNA damage. Mol Cell Biol 2000;20:7751–63.
[34] Kaufmann SH. Cell death induced by topoisomerase-targeted drugs: more questions than answers. Biochim Biophys Acta 1998;1400:195–211.
[35] Roos WP, Kaina B. DNA damage-induced cell death by apoptosis. Trends Mol Med 2006;12:440–50.
[36] Sinkule JA. Etoposide: a semisynthetic epipodophyllotoxin. Chemistry, pharmacology, pharmacokinetics, adverse effects and use as an antineoplastic agent. Pharmacotherapy 1984;4:61–73.
[37] Huang Y, Chan AM, Liu Y, Wang X, Holbrook NJ. Serum withdrawal and etoposide induce apoptosis in human lung carcinoma cell line A549 via distinct pathways. Apoptosis 1997;2:199–206.
[38] Chiu CC, Li CH, Ung MW, Fuh TS, Chen WL, Fang K. Etoposide (VP-16) elicits apoptosis following prolonged G2-M cell arrest in p53-mutated human non-small cell lung cancer cells. Cancer Lett 2005;223:249–58.
[39] Facompré M, Wattez N, Kluza J, Lansiaux A, Bailly C. Relationship between cell cycle changes and variations of the mitochondrial membrane potential induced by etoposide. Mol Cell Biol Res Commun 2000;4:37–42.
[40] Lee SB, Tong SY, Kim JJ, Um SJ, Park JS. Caspase-independent autophagic cytotoxicity in etoposide-treated CaSki cervical carcinoma cells. DNA Cell Biol 2007;26:713–20.
[41] Eisenberg T, Knauer H, Schauer A, Büttner S, Ruckenstuhl C, Carmona-Gutierrez D, et al. Induction of autophagy by spermidine promotes longevity. Nat Cell Biol 2009;11:1305–14.
[42] Morselli E, Galluzzi L, Kepp O, Criollo A, Maiuri MC, Tavernarakis N, et al. Autophagy mediates pharmacological lifespan extension by spermidine and resveratrol. Aging (Albany NY) 2009;1:961–70.
[43] Crowley LC, Elzinga BM, O'Sullivan GC, McKenna SL. Autophagy induction by Bcr-Abl-expressing cells facilitates their recovery from a targeted or nontargeted treatment. Am J Hematol 2011;86:38–47.
[44] Dunn Jr WA. Studies on the mechanisms of autophagy: formation of the autophagic vacuole. J Cell Biol 1990;110:1923–33.
[45] Overmeyer JH, Kaul A, Johnson EE, Maltese WA. Active ras triggers death in glioblastoma cells through hyperstimulation of macropinocytosis. Mol Cancer Res 2008;6:965–77.
[46] Bhanot H, Young AM, Overmeyer JH, Maltese WA. Induction of nonapoptotic cell death by activated Ras requires inverse regulation of Rac1 and Arf6. Mol Cancer Res 2010;8:1358–74.
[47] Suárez Y, González L, Cuadrado A, Berciano M, Lafarga M, Muñoz A, Kahalalide F. a new marine-derived compound, induces oncosis in human prostate and breast cancer cells. Mol Cancer Ther 2003;2:863–72.
[48] Sperandio S, Poksay K, de Belle I, Lafuente MJ, Liu B, Nasir J, et al. Paraptosis: mediation by MAP kinases and inhibition by AIP-1/Alix. Cell Death Differ 2004;11:1066–75.
[49] Gewirtz DA, Holt SE, Elmore LW. Accelerated senescence: an emerging role in tumor cell response to chemotherapy and radiation. Biochem Pharmacol 2008;76:947–57.
[50] Saretzki G. Cellular senescence in the development and treatment of cancer. Curr Pharm Des 2010;16:79–100.
[51] Rebbaa A. Targeting senescence pathways to reverse drug resistance in cancer. Cancer Lett 2005;219:1–13.
[52] Shay JW, Roninson IB. Hallmarks of senescence in carcinogenesis and cancer therapy. Oncogene 2004;23:2919–33.
[53] Dimri GP. What has senescence got to do with cancer? Cancer Cell 2005;7:505–12.
[54] Chang BD, Broude EV, Dokmanovic M, Zhu H, Ruth A, Xuan Y, et al. A senescence-like phenotype distinguishes tumor cells that undergo terminal proliferation arrest after exposure to anticancer agents. Cancer Res 1999;59:3761–7.
[55] Collado M, Serrano M. Senescence in tumours: evidence from mice and humans. Nat Rev Cancer 2010;10:51–7.
[56] Alimonti A, Nardella C, Chen Z, Clohessy JG, Carracedo A, Trotman LC, et al. A novel type of cellular senescence that can be enhanced in mouse models and human tumor xenografts to suppress prostate tumorigenesis. J Clin Invest 2010;120:681–93.